

## Effects of zinc-based flame retardants on the degradation behaviour of an aerospace epoxy matrix

A. De Fenzo<sup>a,b,\*</sup>, C. Formicola<sup>a,b</sup>, V. Antonucci<sup>a,b</sup>, M. Zarrelli<sup>a,b</sup>, M. Giordano<sup>a,b</sup>

<sup>a</sup>IMCB – Institute of Composite Materials and Biomedical CNR, National Research Council, Piazzale Enrico Fermi, 1 Portici, Napoli, Italy

<sup>b</sup>IMAST – Technological District on Polymeric and Composite Materials Engineering, P. E. Fermi 1, Portici 80055, Italy

### ARTICLE INFO

#### Article history:

Received 21 January 2009

Received in revised form

16 March 2009

Accepted 27 May 2009

Available online 6 June 2009

#### Keywords:

Epoxy

Thermogravimetric analysis

Flame retardants

Degradation kinetics

Cone calorimeter

### ABSTRACT

Flame behaviour is a fundamental requirement for advanced aerospace composites. In this work, a commercial, low-viscosity epoxy system, typically used in liquid infusion composite processes, and its mixtures with three different zinc-based flame retardants (ZB, ZS, ZHS) at different weight percentages has been investigated by cone calorimetry and thermogravimetric analysis.

Cone calorimetry has been performed to verify the flame retardancy effects induced by each filler composition. Nevertheless manufacturability issues require the evaluation of the rheological changes induced by filler on the unloaded matrix system. Rheological tests have been, therefore, performed to identify the maximum concentration of filler. Based on these results thermogravimetric tests have been performed to investigate thermal degradation kinetics of selected systems. The feasibility of Kissinger and Flynn-Wall-Ozawa method for the determination of characteristic degradation kinetics parameters has been evaluated and results were analysed. A simplified decomposition model was assumed to analyse epoxy degradation behaviour; it was found that this model gives appreciable matching with experimental TGA curve trend for neat epoxy whereas for the filled compounds additional stages were assumed to occur.

© 2009 Elsevier Ltd. All rights reserved.

### 1. Introduction

Epoxy resins are largely used in advanced composites to provide elevated mechanical performance, good chemical and electrical resistance, better design flexibility and higher specific properties. Flammability of epoxy resins still represents a limitation for that part of commercial and general aviation aircraft where fire propagation involves both health risks and loss of mechanical properties. To improve fire resistance of epoxy-based composites, the use of phosphorus compounds has been studied. In the condensed phase, these compounds promote char formation which protects the underlying material from heat, at the same time, acting as a barrier

to toxic gas release [1]. Often halogen compounds are used to improve fire resistance of composites, but, in the recent years, those additives have been forbidden due to the highly toxicity and corrosive fumes released during combustion.

Halogen-free compounds were used by Perez et al. [2] as filler for epoxy matrices by chemical synthesis; experimental tests by cone calorimeter and UL94 showed that their action take place by the reduction of one-third of total heat release increasing the residue content of about 5%. The fusion process has been used to realise different mixtures of phosphorus and silicon compounds in different epoxy matrices by Ling et al. [3], reporting that samples, tested under dynamic conditions by TGA, show high char yield at 700 °C in air atmosphere. According to these authors, the formation of the high char yield can be driven by the synergistic effect of phosphorus and silicon additives, with the first enriching the char formation and second acting as protector of the char layer from thermal degradation.

The effect of montmorillonite combined with organophosphorus compounds in the epoxy matrix was studied by cone calorimeter and LOI tests in [4]. The flame retardancy of the epoxy matrix decreases by incorporation of nano-particles of montmorillonite. Those particles have lower mobility due to cross-linking structure which is formed after synthesis with epoxy.

The effect of silica in phosphorus based epoxy systems was studied by TGA dynamic tests in [5,6]. Thermal stability of hybrid

*Abbreviations:* TGA, Thermogravimetric analysis; ZB, Zinc Borate; ZHS, Zinc Hydroxystannate; ZS, Zinc Stannate; ATH, Hydrated alumina; FWO, Flynn-Wall-Ozawa; DTG, Differential Thermal Gravimetry; HRR, Heat Release Rate; TTI, Time To Ignition; VIP, Vacuum Infusion Process; RIFT, Resin Infusion Flexible Tooling; VARTM, Vacuum Assisted Resin Transfer Moulding;  $\alpha$ , Mass loss; T, Temperature;  $\gamma$ , Degree of polymerization or degree of cure;  $\beta$ , Heating rate; R, Gas universal constant;  $T_{max}$ , Peak Temperature of thermal degradation curves;  $n$ , Reaction order;  $p$ , Curve slope;  $E_a$ , Activation energy.

\* Corresponding author. IMCB – Institute of Composite Materials and Biomedical CNR, National Research Council, Piazzale Enrico Fermi, 1 80055 Portici, Napoli, Italy. Fax: +39 0817758850.

E-mail address: [adefenzo@unina.it](mailto:adefenzo@unina.it) (A. De Fenzo).

compound silica/epoxy, in nitrogen and air atmosphere, were also evaluated by peak temperature analysis of DTG curves showing that, in nitrogen atmosphere, the degradation resistance increases by adding silica nano-fillers, while in air flow, a reverse trend was found. Biswas et al. [7] have investigated the degradation behaviour and the evolution of CO and CO<sub>2</sub> gas of epoxy systems in a fire scenario with selected flame retardants as phosphorus compound and halogen based additives. In this case, phosphorus compounds will retard the resin degradation kinetics enhancing char formation at higher temperatures although the combustion reaction remains incomplete.

Flame retardancy of different kinds of thermosets can be ensured by the addition of zinc and tin compounds due to the reduced toxicity and low smoke emission [8–12]. ZS and ZHS act as flame retardants by a combination of different mechanisms in both condensed and vapour phases promoting the formation of char layers [13] at lower temperatures compared with neat polymer. Magnesium hydroxide and alumina trihydrate coated with ZHS and ZS can improve fire resistance, reducing smoke emission at the same time when added to halogenated thermosetting polymers (PVC, Polychloroprene) [14]. ZB is an inorganic salt flame retardant that mixed with a halogen-free polymer significantly reduces heat release rate (HRR) peak, time to ignition (TTI) and smoke evolution [15]. Bourbigot et al. [16] have used ZB in EVA polymer, demonstrating that zinc borate lead to synergistic effects in different formulation with ATH acting as smoke suppressant and generating a vitreous protective layer on the combusted materials [17]. Synergistic effect of ZB with magnesium hydroxide in the ethylene-propylene-diene copolymer has been investigated by cone calorimeter experiments and XRD diffraction [18]. These experiments showed the formation of a very hard char substrate; moreover, heat release was observed to span over a longer period compared to the neat material sample. The same filler has been used with EVA-Mg(OH)<sub>2</sub> copolymer promoting char formation and therefore, delaying the polymer degradation [19].

Among the different modelling methods used to analyse TGA data, Kissinger and Flynn-Wall-Ozawa procedures are generally used as no previous knowledge of the decomposition stages are needed to evaluate activation energy values. Both methods have been already adopted by different authors [20–22] to model the degradation behaviour for neat epoxy resin and also composites. Kandare et al. [23] have reported kinetic studies on different mixtures of epoxy resins and intumescent compounds by modelling the degradation for a specific formulation. Three different stages of degradation were considered, dehydration of resin and additives, cumulative char formation and char oxidation. They also showed that kinetic parameters are substantially independent of mixture composition.

In the present work, a thermogravimetric analysis was carried out on a mono-component high  $T_g$  epoxy system mixed with zinc-based flame retardant compounds at 30% filler concentration. Preliminary tests by cone calorimetry were performed on RTM6 and filled epoxy at different concentrations for each additives (5–10–20–30–40% wt) in order to evaluate the flame retardancy effect induced by the loading content compared with neat matrix. The unloaded RTM6 system, certified for aerospace applications, has been formulated to manufacture composite parts by liquid infusion processes, such as (VIP, RIFT or VARTM) due to its very low viscosity (50 mPa\*s) at infusion temperature. Its inherent value of viscosity assures the complete impregnation of the reinforcing mat under the action of positive pressure or vacuum. The increase of viscosity, due to high filler contents, would lead to unacceptable values of injection pressure and in some case, to complete un-processability of the system by liquid moulding. For these reasons, a specific concentration (30%) was chosen according to rheological changes for the

investigation of decomposition kinetics of each filler. Two different modelling methods (Kissinger and FWO) were implemented at the same loading concentrations by comparing onset temperatures and mass loss percentages respectively in both air and nitrogen atmosphere. Zinc compounds induce the formation of a higher char yield and additional quantity of residue compared to the neat resin, mainly at lower temperature. The activation energy computed by Kissinger and Ozawa methods shows a multistage mechanism of degradation especially in air flow. Analysis based on dynamic TGA scans show that for ZHS compounds, in nitrogen flow, report two different decomposition step while for ZB and ZS filled system and neat epoxy material a single stage degradation is observed. The simple decomposition model according to Rose et al. has been considered to analyse the experimental data considering additional steps to correctly interpret ZHS decomposition curve.

## 2. Materials

The material investigated was the HexFlow<sup>®</sup> RTM6 mono-component epoxy resin specifically developed to fulfil the requirements of the aerospace industries in advanced resin transfer moulding or infusion. RTM6 is a premixed epoxy system for service temperatures from –60 °C up to 200 °C with an uncured and a fully cured state glass transition respectively of –10 °C and 185 °C. At room temperature, it is a brown translucent paste but its viscosity decreases quickly with increasing temperature up to a minimum ~50 mPa\*s making this system very suitable for infusion processes. The flame retardants used in this work were three different zinc-based compounds supplied by Joseph Storey Company, zinc borate, zinc stannate and zinc hydroxystannate.

## 3. Experimental

Light microscopy analysis of zinc compounds and mixed epoxy system are carried out with an OLYMPUS BX51 microscope at 50× magnification in order to evaluate the average dimension of the micro particles. The mixing of flame retardants into the epoxy matrix was performed by mechanical stirring (Heidolph RZR equipment) using two different step rates (1050 and 2000 rpm) process with various weight concentration of zinc salt (5–10–20–30–40% wt) for 30 min. After mixing, the system was degassed at 90 °C for 1 h; then cured by a two-step dwell temperature profile (1.5 h at 160 °C and 2 h at 180 °C). Cone calorimeter tests were performed using a Fire Testing Technology Ltd. cone calorimeter according to the ASTM E1354-04 procedure.

Samples for all the percentages of the considered fillers, with nominal dimensions of 100 × 100 × 3 mm, were tested horizontally under an irradiating flux of 50 kW/m<sup>2</sup>. Samples taken from fully cured panel were, then, scanned by a TA Instruments 2950 TGA under dynamic conditions with temperature ramps of 5–7.5–10 and 20 °C/min from ambient to 800 °C, in inert and oxidant atmosphere.

## 4. Analytical modelling

For dynamic TGA measurements, mass loss is monitored as function of temperature at different heating rates. Kinetics of degradation in the general form can be modelled as:

$$\frac{d\alpha}{dt} = f(\alpha, T) \quad (1)$$

where  $T$  and  $\alpha$  represents respectively, temperature and mass loss. Considering an  $n$ th order reaction mechanism and the degradation

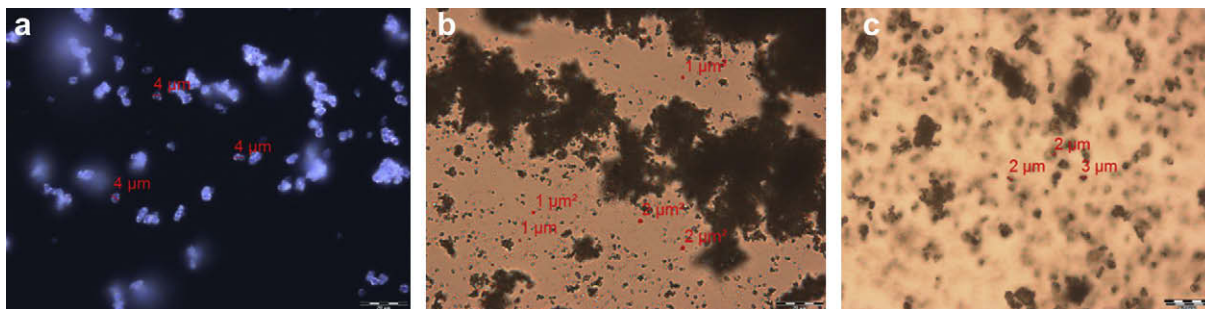


Fig. 1. Light microscopy of zinc-based powder as received – a) ZB, b) ZHS, c) ZS.



Fig. 2. Light microscopy of 20% wt fully cured samples – a) RTM6 + ZB, b) RTM6 + ZHS, c) RTM6 + ZS.

rate following Arrhenius temperature dependence, it can be written:

$$\frac{d\alpha}{dt} = K(T)f(\alpha) \tag{2}$$

with

$$k = A \exp\left(\frac{-E}{RT}\right) \tag{3}$$

The combination of (2) and (3) gives

$$\frac{d\alpha}{dt} = Af(\alpha)\exp\left(\frac{-E}{RT}\right) \tag{4}$$

If heating rate  $\beta = dT/dt$  is constant, the variation in degree of conversion can be analysed as a function of temperature and, this temperature being dependent on the time of heating:

$$\frac{d\alpha}{dT} = \frac{A}{\beta} f(\alpha) \exp\left(\frac{-E}{RT}\right) \tag{5}$$

The integrated form of this equation generally is expressed as:

$$g(\alpha) = \int_0^\alpha \frac{d\alpha}{f(\alpha)} = \frac{A}{\beta} \int_0^T \exp\left(\frac{-E}{RT}\right) dT \tag{6}$$

where  $g(\alpha)$  is the integrated form of the conversion dependence function.

Two different methods (differential and integral) were applied in this work: Kissinger and Flynn-Ozawa method. The first method allows the determination of activation energy without a precise

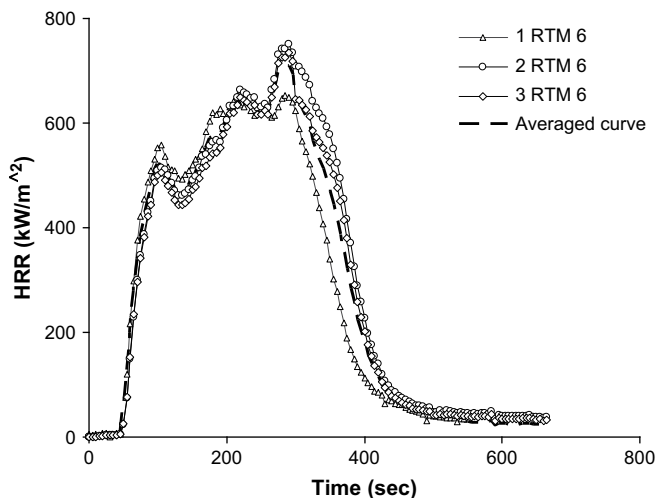


Fig. 3. Cone calorimeter tests for the neat RTM6 epoxy system.

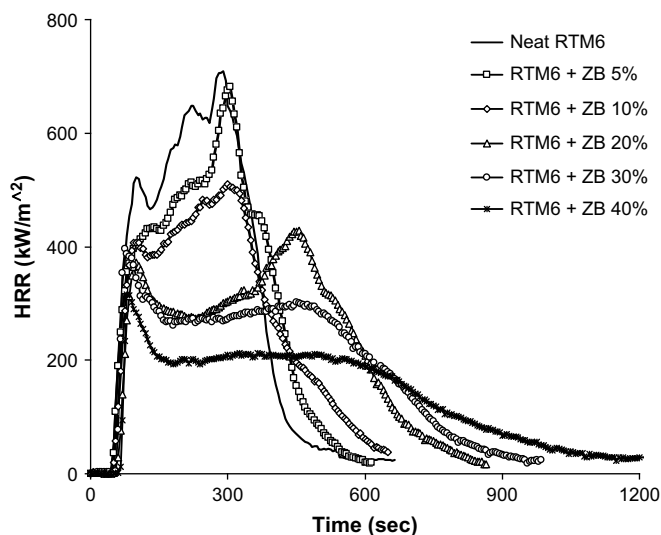


Fig. 4. Cone calorimeter curves for ZB mixture at different concentrations.

knowledge of the reaction mechanism. It analyzes the variations in the thermogravimetric data through the changes of run heating rate,  $\beta$ , as function of the maximum peak temperatures,  $T_{\max}$  (in DTG curves) according to the following equation:

$$\ln\left(\frac{\beta}{T_{\max}^2}\right) = \left\{ \ln\frac{AR}{E} + \ln\left[n(1 - \alpha_{\max})^{n-1}\right] \right\} - \frac{E}{RT_{\max}} \quad (7)$$

where  $T_{\max}$  is the temperature of inflection point of thermal degradation curves which corresponds to the maximum reaction rate;  $\alpha_{\max}$  is the conversion at  $T_{\max}$ , and  $n$  is the reaction order. Assuming that  $f'(\alpha_{\max}) = n(1 - \alpha_{\max})^{n-1} \cong \text{const.}$  the activation energy  $E$  can be determined from a plot of  $\ln(\beta/T_{\max}^2)$  against  $1/T_{\max}$ .

By Flynn-Wall-Ozawa method it is possible to estimate the values of activation energy applying Doyle's approximation [23] integrating eq. (6). It can be written:

$$\log \beta = \log \left[ \frac{AE}{g(\alpha)R} \right] - 2.315 - 0.4567 \frac{E}{RT} \quad (8)$$

Iso-conversion curves can be obtained by plotting  $\log \beta$  vs.  $1/T$  and the  $p$  slope of the straight lines can be correlated with activation energy as follows:

$$p = -0.4567 \frac{E}{RT} \quad (9)$$

Compared to others, the Kissinger and Flynn-Wall-Ozawa methods present the advantage that they do not require previous knowledge of the reaction mechanism for determining the activation energy.

## 5. Results and discussion

### 5.1. Optical microscopy

Optical micrographs of zinc-based flame retardants, as received, are reported in Fig. 1. Average particle size was evaluated for all three additives by the freely available image analysis program *ImageJ*. It was found that ZB shows, on averaging basis, a coarser granulometry compared with tin-based compounds. An average size of  $4 \mu\text{m}$  was measured compare to the  $2 \mu\text{m}$  of tin compound (Fig. 1). A uniform dispersion of additives for all mixtures was obtained as shown in Fig. 2.

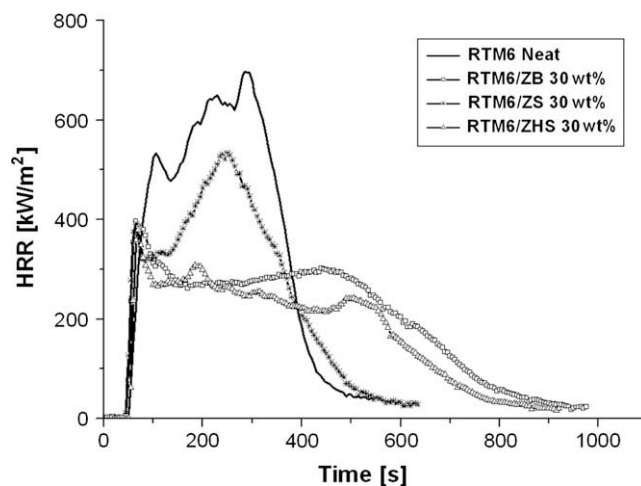
### 5.2. Cone calorimetry

Fig. 3 reports fire curves obtained for the neat resin samples by cone equipment over three different tests along with the averaged values. These curves show a good repeatability of the trend with a slight deviation of combustion behaviour at the post-flash over point (decay region) with an almost constant end-of-test time. Cone calorimeter curves, for all considered concentrations for ZB loaded mixture are reported in Fig. 4. As expected, higher enhancements of fire retardancy are associated to a higher

**Table 1**

Characteristic cone calorimeter parameters for ZB loaded resin at different percentages.

Sample	TTI (s)	pHRR (kW/m <sup>2</sup> )	HRR average (kW/m <sup>2</sup> )
RTM6 neat	43 ± 2	702 ± 6	382 ± 6
RTM6 + ZB 5 wt%	44 ± 5	682 ± 7	354 ± 4
RTM6 + ZB 10 wt%	44 ± 2	523 ± 5	265 ± 5
RTM6 + ZB 20 wt%	49 ± 3	428 ± 6	251 ± 3
RTM6 + ZB 30 wt%	57 ± 2	396 ± 5	193 ± 4
RTM6 + ZB 40 wt%	68 ± 4	315 ± 8	148 ± 3



**Fig. 5.** Cone curves for zinc-based filler and epoxy resin system mixture for 30% wt.

concentration of filler. In fact, the flame out is gradually increased to higher values for major loading content (from 553 s for the neat system to 1200 s for the 40% wt loadings).

Data reported in Table 1 show that a progressive variations of pHRR and HRR average from 5% to 40% filler content, with a maximum change of about 50% (from 382 to 148 kW/m<sup>2</sup>) in the case of 40% wt. It can be noticed, that, in Fig. 4 the HRR peak of RTM6/ZB 5 wt% is relatively high compared to the trend associated with neat resin and 10% wt loadings (see circled area in Fig. 4). This curve's behaviour could be attributed to a local instability of the heat flux during the test leading to a wider cracked area and therefore, a localised combustion growth. Analogous test were performed for the ZHS and ZS fillings at the same weight concentrations. Although the maximum considered concentration (40% wt) induces better flame behaviour of the loaded epoxy system, a weight content of 30% was fixed for the degradation analysis by thermogravimetric analysis (TGA). This filler percentage has been selected since greater contents increase significantly the resin viscosity and, hence, limiting its processability. In fact, the RTM 6 is one of the most used matrix for the manufacturing of advanced reinforced composites by infusion processes (VIP, RIFT or VARTM) which requires low viscosity values (not exceeding 500–600 mPa\*s). Fig. 5 reports for completeness purpose, the averaged curves of cone calorimeter analysis performed on 30% wt filled system superimposed with neat epoxy material. Main parameters extracted from these curves, show that almost the same TTI values characterise the different systems within the reproducibility error range. Decreasing values for the pHRR and HRR average are reported for all filled system compared to the neat RTM6, with a maximum change respectively of 323 kW/m<sup>2</sup> and 190 kW/m<sup>2</sup> for the ZHS loading (Table 2).

### 5.3. Thermogravimetric analysis (TGA)

Fig. 6 shows respectively the thermogravimetric data of neat epoxy resin in inert flow at different heating rates and the

**Table 2**

Characteristic parameters for 30% wt loaded mixtures obtained by cone calorimeter curves shown in Fig. 5.

Sample	TTI (s)	pHRR (kW/m <sup>2</sup> )	HRR average (kW/m <sup>2</sup> )
RTM6 neat	43 ± 2	702 ± 7	382 ± 5
RTM6 + ZB 30 wt%	47 ± 3	396 ± 5	193 ± 6
RTM6 + ZHS 30 wt%	52 ± 4	379 ± 4	192 ± 4
RTM6 + ZS 30 wt%	43 ± 3	551 ± 8	274 ± 8



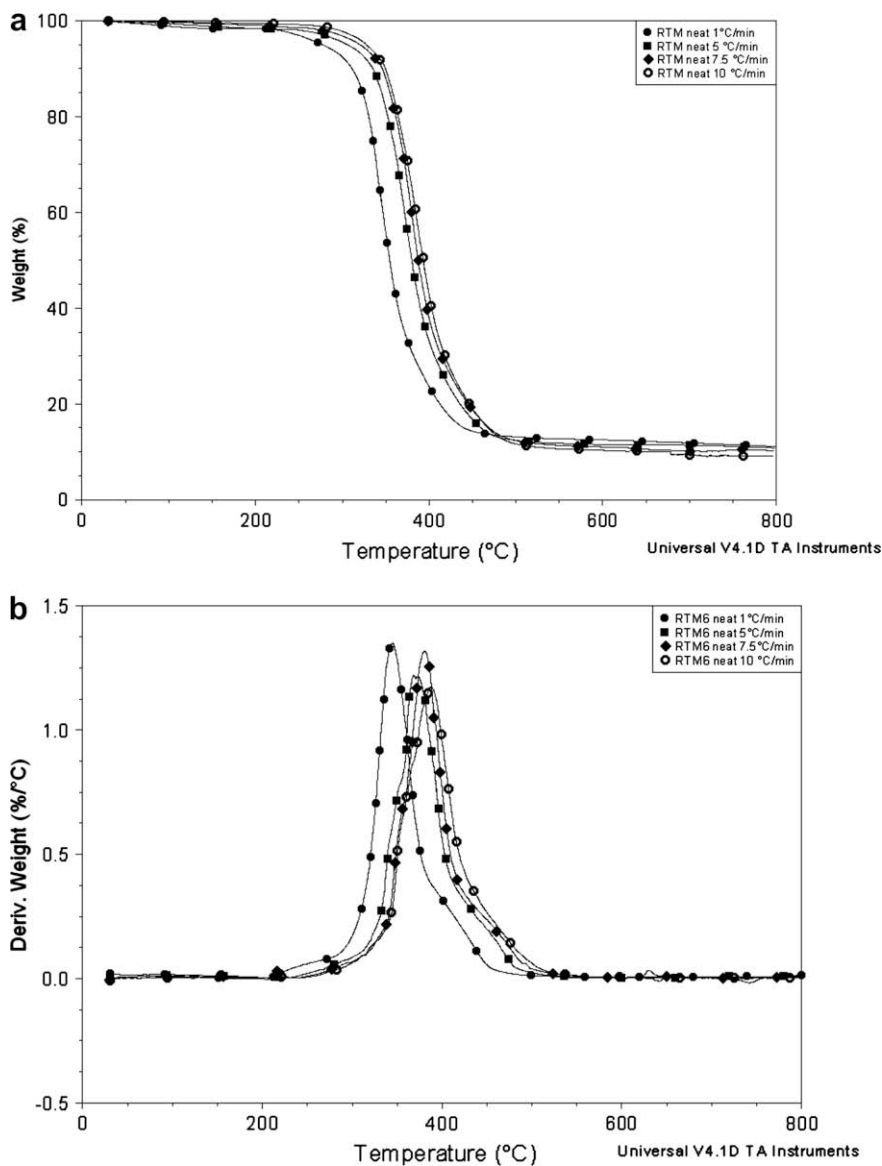


Fig. 6. Thermogravimetric measurements in the epoxy resin neat in the inert flow.

corresponding DTG curves. Mass is lost with increasing temperature rate yielding earlier degradation onsets. It can be noticed that, neat epoxy resin shows only one step of degradation with an initial degradation onset between 314 °C and 350 °C with a mass lost respectively of 13.1% and 9.2% for experiments run from 1 to 10 °C/min (Table 3). DTG curves show that maximum peak temperatures are slightly dependent upon heating rates. Initial degradation onset and maximum peak temperatures are reported in Table 3 at each heating ramps.

Degradation behaviour of the neat epoxy was also studied in oxidant atmosphere and corresponding TGA and DTG curves are reported in Fig. 7a and b. While in nitrogen flow, char yield

**Table 3**  
Reference temperatures after TG measurements for neat RTM6, in nitrogen.

Heating rate (°C/min)	$T_{\text{onset}}$ (°C)	Mass loss (%)	$T_{\text{peak max}}$ (°C)
1	314	11.1	341
5	342	13.1	368
7.5	350	12.2	381
10	347	9.2	387

obtained at 800 °C is dependent on heating rate, in oxidant atmosphere, the mass loss is total at 700 °C for all considered temperature rates. Moreover, under these conditions, two different degradation steps, spanning the whole investigated temperature range, are traceable. The first degradation step is located in the range 200–430 °C with a slight deviation for all heating rates, whereas the second step (charring stage) is characterised by an almost constant starting temperature at 500 °C with an end-decomposition offsets between 565 °C and 700 °C with increasing rates. The mass loss during the charring stage was about 40% and, as expected, it is not a function of the heating ramps. A transition region between the two steps can be identified in the range 400–500 °C with mass loss curves substantially independent by the heating rates. Initial degradation onset and maximum peak temperatures under air flow, are reported respectively in Table 4.

The simplified decomposition model by Rose and co-workers [24,25] 1) epoxy resin ( $m_1$ ) → dehydrogenated epoxy ( $m_2$ ) + water; 2) dehydrogenated epoxy ( $m_2$ ) → stable carbonaceous char ( $m_3$ ) + volatiles; 3) stable carbonaceous char ( $m_3$ ) → volatiles could be very useful to elucidate the physical phenomena underlying the

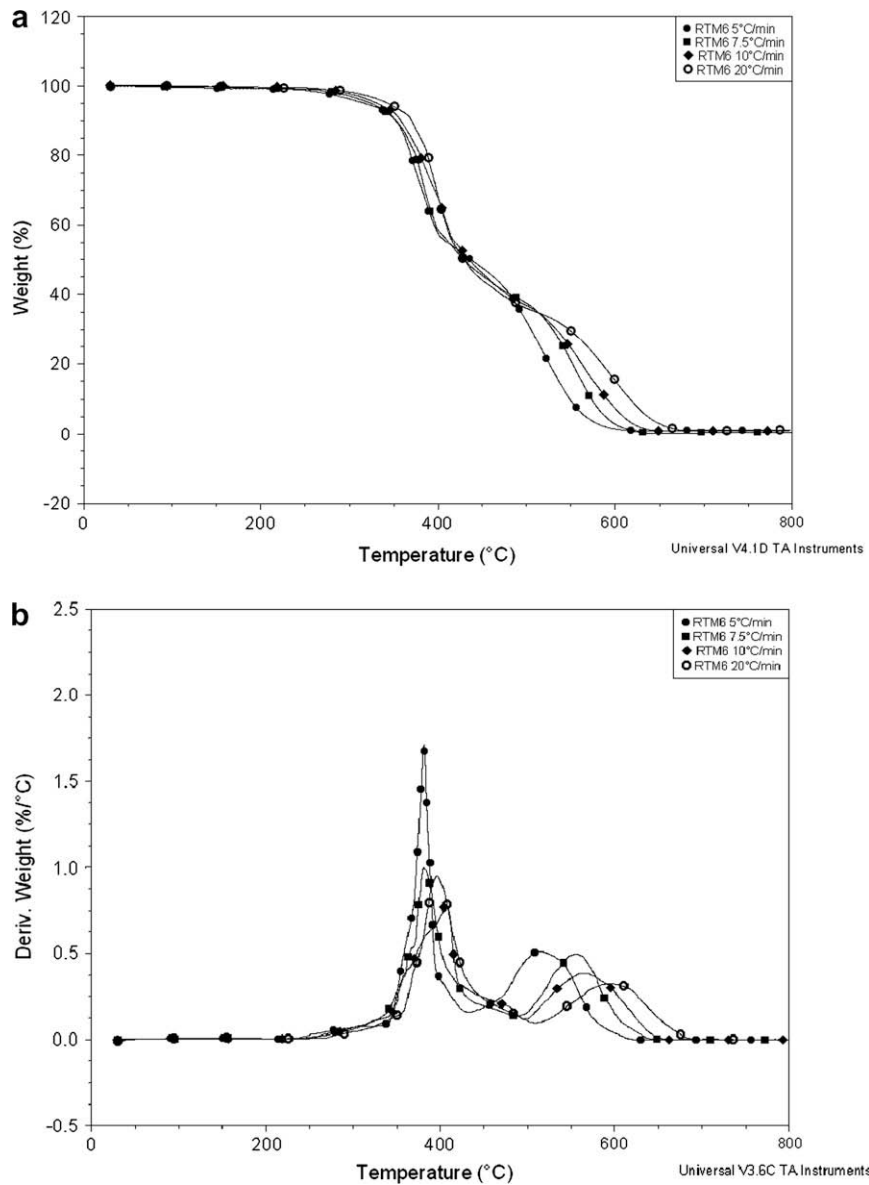


Fig. 7. Thermogravimetric data collected in air atmosphere for RTM6 neat.

**Table 4**  
Reference temperature after TG measurements for neat RTM6, in air flow.

Heating rate (°C/min)	$T_{onset}$ (°C)	Mass loss (%)	$T_{peak\ max}$ (°C)
I step			
1	347	8.1	381
5	357	10.3	384
7.5	358	11.2	405
10	370	13.5	407
II step			
1	481	60.3	512
5	524	68.6	556
7.5	529	69.5	561
10	551	70.5	594

**Table 5**  
 $T_{max}$  values obtained from DTA scans performed on loaded resin system.

Sample	Heating rate °C/min	$T_{max}$ (°C)					
		Nitrogen		Air			
		I step	II step	I step	II step	III step	IV step
ZB	5	379		372	508		
	7.5	385		399	509		
	10	392		400	524		
	20	408		418	547		
ZHS	5	227	353	265	353	380	494
	7.5	233	360	270	360	382	514
	10	235	365	272	362	385	511
	20	240	376	282	372	417	545
ZS	5	354		353	371		498
	7.5	362		358	393		502
	10	367		363	395		514
	20	377		373	398		546

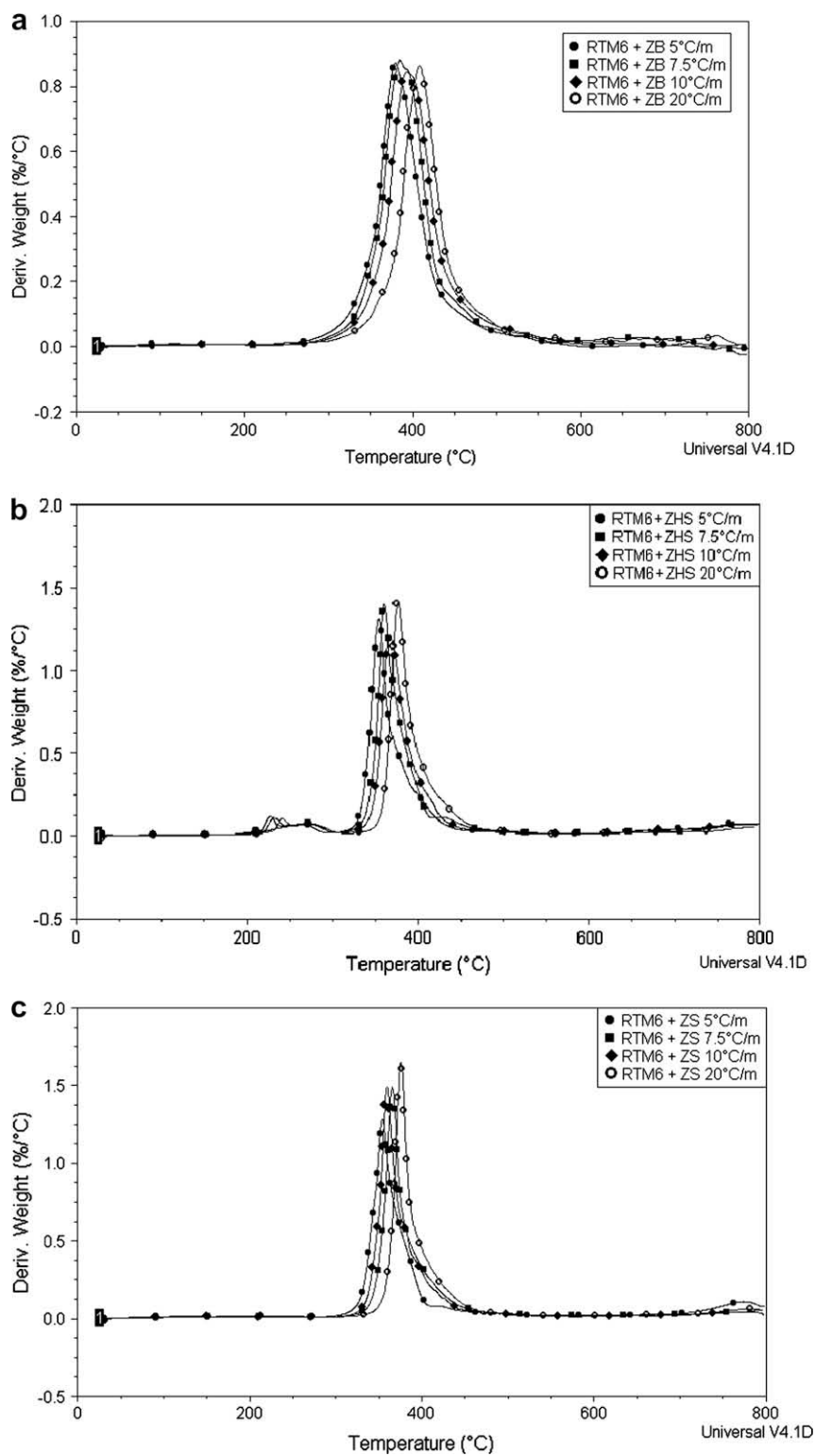


Fig. 8. DTG curves for RTM 6 loaded with 30% wt ZB a), ZHS b), ZS c) under nitrogen flow.

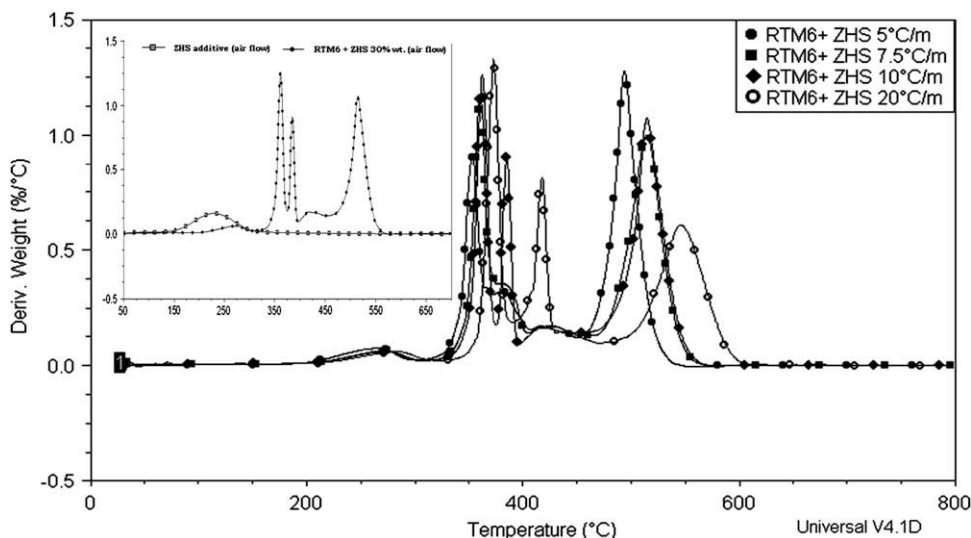


Fig. 9. DTG measurements for RTM 6 loaded with 30% wt ZHS under air flow.

decomposition curve trend. In the range 25–300 °C, the system is dehydrated (*m1*) with an amount of released water of about 1.1% leading to the formation of a moisture-free resin system (*m2*). Next, the decomposition in stable carbonaceous (*m3*) char and different volatile species takes place in the range 300–430 °C. The dehydration and the stable char formation reactions could reasonably be assumed to model the first curve step. The third reaction is responsible for the further degradation of the stable carbonaceous char (*m3*) to competition leaving no residue above 700 °C. The superposition of the two last reactions, stable char formation (*m2*) and its total degradation (*m3*), could be considered as logical explanation for the long-lasting transition region which appears substantially independent by the heating rates.

The difference in degradation behaviour of the epoxy resins containing various flame retardant loadings could be clearly read from the differential thermogravimetric (DTG) thermograms. Based on the number of peaks in DTG curves, the weight loss processes of the mixtures were considered as several stages. Table 5 reports the values of  $T_{max}$  for each filler in both inert and air atmosphere. In Fig. 8a–c, the DTG signals for RTM6 system mixed respectively with ZB, ZHS, ZS at 30% wt. are shown for the case of inert flow. It can be noticed that, only samples obtained by mixing RTM6 with zinc hydroxystannate show two different steps of degradation respect to the single step trend reported by ZB and ZS loaded compounds. For both steps located respectively, around 270 °C and 370 °C with a corresponding mass loss of about 10% and 55%, the dependency on the heating rates is maintained over the whole examined temperature range. A right shift of all curves at increasing rates is observed.

Table 6  
Apparent activation energy according to the Kissinger analysis.

Purge gas	Sample	Ea (KJ/mol)			
		I step	II step	III step	IV step
Nitrogen	RTM6	154	–	–	–
	RTM6+ZS	158	–	–	–
	RTM6+ZHS	91	86	–	–
	RTM6+ZB	153	–	–	–
Air	RTM6	82	116	–	–
	RTM6+ZS	223	115	135	–
	RTM6+ZHS	187	217	472	127
	RTM6+ZB	147	180	–	–

All samples were investigated also in air atmosphere. Fig. 9 reports RMT6/ZHS derivative curves for 5–7.5–10–20 °C/min heating rates. Obtained results show different stages of degradation according to the type of filler and particularly for the RTM6+ZHS, four steps can be discerned (Fig. 9).

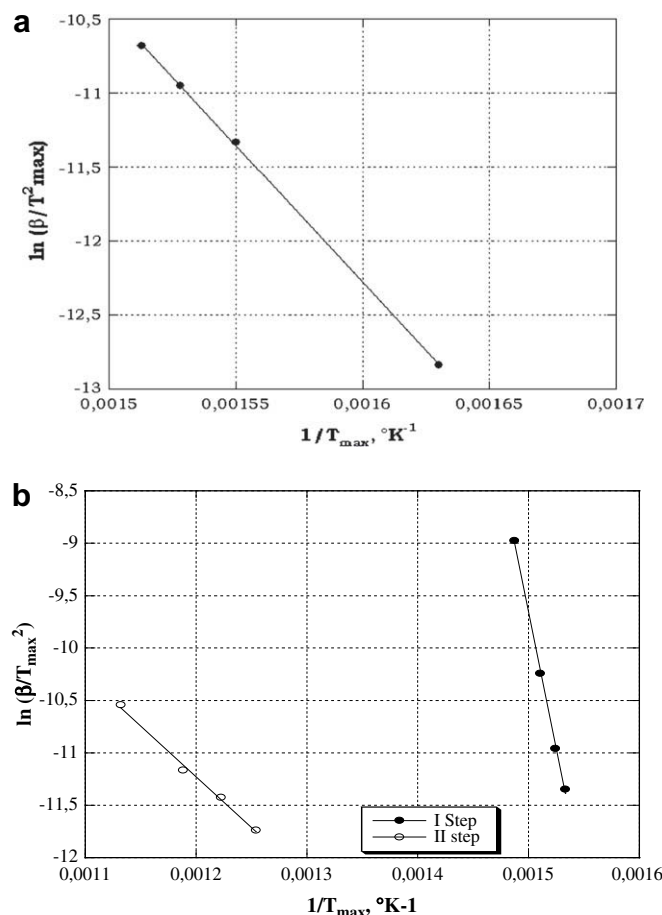


Fig. 10. Kissinger graphs for RTM6 data in a) inert and b) air atmosphere.



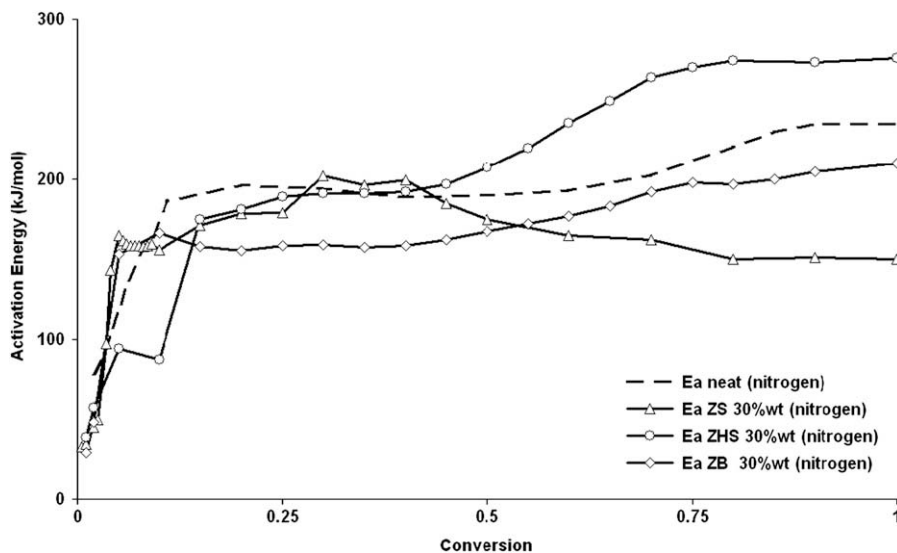


Fig. 11. Activation Energy results computed by Ozawa method for RTM6 neat and its mixtures at 30 wt (nitrogen).

In the first stage, resin is dehydrated and an amount of water of about 1% of the original weight is removed leading to the formation of moisture-free polymer system. Crystallization water molecules associated to ZHS are released with a mass loss of 5% between 180 °C and 230 °C. This temperature range is lower if compared with TGA mass loss of neat ZHS sample (reduced Fig. 9) due to the earlier stage undergone by filled epoxy to achieve full polymerization conversion ( $T = 180$  °C, 90 min). Between 300 °C and 400 °C two different mechanisms take places probably due to the presence of intermediate products yielding to the formation of unstable carbonaceous structure which degrades completely during the final stage.

#### 5.4. Kissinger and Ozawa model results

Kissinger method (eq. (7)) was employed for all TGA scans performed on neat resin system and all 30% wt filled mixtures, in

order to evaluate the activation energy of each degradation step in air and nitrogen. Table 6 summarizes all calculated values. Fig. 10 a) and b) reports Kissinger  $\ln(\beta/T_{max}^2)$  vs.  $1/T_{max}$  curves for each identified degradation stage, for untreated resin.

In nitrogen, activation energy values are substantially constant for ZB (153 kJ/mol) and ZS (158 kJ/mol) mixtures compared with neat epoxy (154 kJ/mol). On the other hand, the presence of ZHS not only leads to two different degradation steps, but also reduces the apparent energy values of more that 40% compared with original polymer. These experimental observations could be drawn out for all TGA curves at considered heating rates. The RTM6/ZHS first degradation stage, characterised by 91 kJ/mol activation energy, can be associated with initial dehydrogenation mass loss of ZHS additive occurring over the range 180–200 °C. It can be supposed that degradation process of the resin is delayed by the presence of ZHS as the energy level related with the chain scission (char formation) can not be achieved at same temperatures as in the case

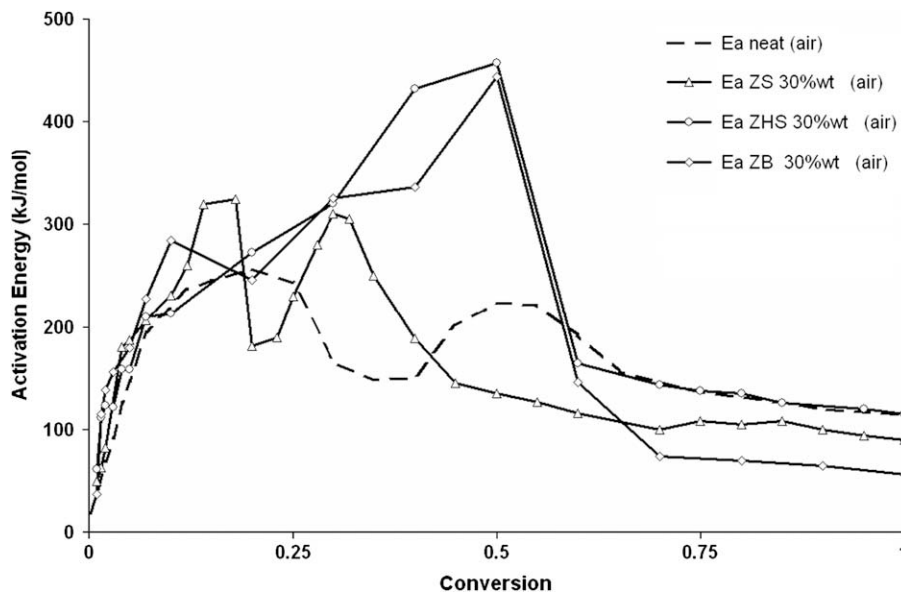


Fig. 12. Activation Energy results computed by Ozawa method for RTM6 neat and its mixtures at 30 wt (air).

of unloaded resin. Therefore, a further decomposition stage (86 kJ/mol), at higher temperatures, will occur to form stable carbonaceous char. For the ZB-based filler (and ZS), activation energy is substantially the same value of unloaded resin highlighting the fact that an identical mechanism of degradation occurs. In air flow for the neat system, the two activation energy values, corresponding to the degradation stages are lower (82 kJ/mol and 116 kJ/mol) compared with the single step obtained under nitrogen flow (154 kJ/mol). A double step degradation is also predicted in the case of RTM6/ZB with two different activation energy values (147 kJ/mol and 180 kJ/mol) which in turn are higher compared with the characteristic levels modelled for the neat resin. ZHS and ZS mixtures show not only multiple stages but also higher  $E_a$  values for each step compared with the neat resin system. These later results suggest a different comprehensive degradation mechanism in which more oxidative stages are involved. The FOW integral analysis, based on eq. (9), was also carried out to evaluate the dependence of apparent activation energy over the extent of reaction. Modelling results are considered for comparison purposes because the Kissinger method accounts only for one point of thermal degradation curve whereas the FOW model considers different points, each corresponding to different conversion values. In Figs. 11 and 12, the energy profiles, over the whole conversion range, are presented for neat RTM6 epoxy and all filled system, respectively for nitrogen and air atmosphere.

In inert flow for all curves, an almost constant value for  $E_a$  was found within the range 10–55% conversion with an increasing trend of the curve at lower percentages (0–10%) as the degradation reaction is triggered. The activation energy values also tend to increase at higher conversion (>55%) for ZHS and ZB presumably due to the formation of a more stable carbonaceous char which delays the overall degradation; whereas a gradual reduction of  $E_a$  value is recorded for ZS-based samples. Under oxidant atmosphere, when 20% mass is lost, the energy curve increases as the decomposition gradually takes place for all the loaded mixtures. However, while for RTM6 and RTM6/ZB mixture a double oscillating profile ranging respectively from 250 kJ/mol to 170 kJ/mol and from 320 kJ/mol to 190 kJ/mol is observed, for the ZHS and ZS mixtures a gradually growing trend is recorded. For higher values of conversion ( $\gamma > 60\%$ ), all activation energy profiles are characterised by a negative derivative path toward full conversion. However, for the RTM6 and RTM6/ZS systems the rate trend is regular and smooth whereas for ZHS and ZB loaded mixtures an abrupt drop is reported. A possible explanation for these different trends, during the final stage of degradation, could be found either for RTM6/ZB considering the stable and compact residue layer which delays the last degradation stage ( $m_3$ ) and for the RTM6/ZHS assuming that the three earlier stages of the degradation process (DTG curves in Fig. 9b) occur at higher energy levels.

## 6. Conclusions

The thermal stability of an epoxy resin mixed with zinc-based flame retardants was investigated by thermogravimetric measurements. Preliminary tests by cone calorimetry at different weight content (from 5 to 40%) were used to verify the flame retardancy effects induced by the different percentages of each filler. Although, it was found that higher load content (40%) assures a lower heat release rate (HRR) value, a fixed composition of 30%

weight for each considered additive was used for the later TGA degradation analysis. The main reason is associated with the detrimental effects induced by high filler content on chemo-rheological behaviour of the matrix. Analyses based on dynamic TGA scans show that for ZHS compounds, in nitrogen flow, show two different decomposition steps while for the ZB and ZS filled system and neat epoxy material a single stage process which characterised degradation behaviour, is observed. The simple decomposition model according to [24,25] has been considered to analyse experimental curves. This model can be reasonably used to describe the curve trend identifying the main decomposition mechanisms and related products. In the case of ZHS (in oxidant flow) an additional decomposition stage is needed to account for release of water of crystallization in the temperature range 180 °C–200 °C. According to the Kissinger analysis, the following conclusions can be drawn.

- in the case of ZHS loaded compounds, decomposition curves show a pre-stage of degradation around 200 °C characterised by an apparent activation energy, 50% lower than neat resin (in the inert flow)
- the same activation energy found for neat system, can be evaluated for the ZB and ZS filled epoxy (inert flow).
- the computation of more energy values in the case of ZHS is in accordance with previous analysis of TGA curves, highlighting the presence of multiple stages of degradation characterised by higher activation energy compared with neat epoxy. (air flow)

Activation energy values, computed by FWO model, make it clear that different decomposition stages are gradually triggered over the whole range of conversion: an extensive superposition of various degradation stages is believed to occur, in the case of ZHS and ZB (air flow), leading to crescent-like profile; while separate mechanism steps can be accounted for ZS filler, giving an oscillating activation energy profile similarly to the neat epoxy system.

## References

- [1] Hergenrother PM. *Polymer* 2005;46:5012–24.
- [2] Perez RM. *J Mater Sci* 2006;41:4981–4.
- [3] Ling LY, Chiu YC, Wu CS. *J Appl Polym Sci* 2002;87:404–11.
- [4] Toldy A, Toth N, Anna P, Marosi G. *Polymer Degrad Stab* 2006;91:585–92.
- [5] Liu YL, Wei WL, Hsu KY, Ho WH. *Termochim Acta* 2004;412:139–47.
- [6] Zong R, Hu Y, Wang S, Song L. *Polym Degrad Stab* 2004;83:423–8.
- [7] Biswas B, Kandola B, Horrocks AR, Price D. *Polym Degrad Stab* 2007;92:765–76.
- [8] Kandare E, Kandola B, Staggs JEJ. *Polym Degrad Stab* 2007;92:1778–87.
- [9] Cusack PA, Hornsby PR. *J Vinyl Addit Technol* 1999;5:21–30.
- [10] Atkinson PA, Haines PJ, Skinner GA. *Polym Degrad Stab* 2001;71:351–60.
- [11] Wu S, Cong P, Yu J, Luo X, Mo L. *Fuel* 2005;85:1298–304.
- [12] Wu Z, Shu W, Hu Y. *J Appl Polym Sci* 2006;103:3667–74.
- [13] Fontaine G, Bourbigot S, Duquesne S. *Polym Degrad Stab* 2008;93:68–76.
- [14] Petsom A, Roengsumran S. *Polym Degrad Stab* 2002;80:17–22.
- [15] Hornsby PR, Cusack PA. *J Mater Sci* 2003;38:2893–9.
- [16] Shen KK, Kochesfahani S, Jouffret F. *Polym Adv Tech* 2008;19:469–74.
- [17] Bourbigot S, Le Bras M. *Polym Degrad Stab* 1999;64:419–25.
- [18] Cross MS, Cusack PA, Hornsby PR. *Polym Degrad Stab* 2003;79:309–18.
- [19] Genovese A, Shanks RA. *Polym Degrad Stab* 2007;92:2–13.
- [20] Carpentier F, Bourbigot S, Le Bras M, Delobel R. *Polym Degrad Stab* 2000;69:83–92.
- [21] Wang Q, Shi W. *Polym Degrad Stab* 2006;91:1747–54.
- [22] Chiang CL, Ma C, Wang F, Kuan H. *Eur Polym J* 2003;39:825–30.
- [23] Regnier N, Fontaine S. *J Therm Anal Calorim* 2001;64:789–99.
- [24] Rose N, Le Bras M, Delobel R, Costes B, Henry Y. *Polym Degrad Stab* 1993;42:307–16.
- [25] Rose N, Le Bras M, Bourbigot S, Delobel R. *Polym Degrad Stab* 1994;45:387–97.